FLIGHT TEST OF AN ADAPTIVE CONTROLLER AND SIMULATED FAILURE/DAMAGE ON THE NASA NF-15B

Mark Buschbacher
Aerospace Engineer, Flight Controls and Dynamics
NASA Dryden Flight Research Center
Telephone: 661-276-3838 E-mail: mark.buschbacher@nasa.gov

Heather Maliska
Aerospace Engineer, Structural Loads
NASA Dryden Flight Research Center
Telephone: 661-276-2843 E-mail: heather.a.maliska@nasa.gov

ABSTRACT

The method of flight-testing the Intelligent Flight Control System (IFCS) Second Generation (Gen-2) project on the NASA NF-15B is herein described. The Gen-2 project objective includes flight-testing a dynamic inversion controller augmented by a direct adaptive neural network to demonstrate performance improvements in the presence of simulated failure/damage. The Gen-2 objectives as implemented on the NASA NF-15B created challenges for software design, structural loading limitations, and flight test operations.

Simulated failure/damage is introduced by modifying control surface commands, therefore requiring structural loads measurements. Flight-testing began with the validation of a structural loads model. Flight-testing of the Gen-2 controller continued, using test maneuvers designed in a sequenced approach. Success would clear the new controller with respect to dynamic response, simulated failure/damage, and with adaptation on and off. A handling qualities evaluation was conducted on the capability of the Gen-2 controller to restore aircraft response in the presence of a simulated failure/damage. Control room monitoring of loads sensors, flight dynamics, and controller adaptation, in addition to postflight data comparison to the simulation, ensured a safe methodology of buildup testing. Flight-testing continued without major incident to accomplish the project objectives, successfully uncovering strengths and weaknesses of the Gen-2 control approach in flight.

ACRONYMS AND SYMBOLS

ARTS	Airborne Research Test System
BL	Butt line
CAT	Choose-A-Test
DAG	Dial-A-Gain
DFRC	Dryden Flight Research Center
DLL	Design limit load
FC	Flight condition
FS	Fuselage station
Gen-2	Second Generation (referring to the direct adaptive controller)
IDEEC	Improved digital electronic engine controller
IFCS	Intelligent Flight Control System
IPE	Increased performance engine
NN	Neural network
NWS	Nosewheel steering
PAL	Pick-A-Limit
PID	Proportional, integral, and derivative
PIO	Pilot-Induced oscillation
PVI	Pilot-Vehicle interface
P/Y	Pitch/yaw
SCE-3	Standard Computing Element-3
SE	Sensor
SLMV	Structural loads model validation
STOL	Short takeoff and landing
WL	Water line
WUT	Windup turn

A	Stability state matrix
B	Control state matrix
$\dot{\beta}$	Angular rate of sideslip
b	NN input signal vector
ε	Small bias
G	Adaptation gain
i	Vector index
k	Time frame index
K_p	NN adaptation proportional gain
K_i	NN adaptation integral gain
L	Learning rate
p	Roll rate
p_{basis}	NN roll axis control input
q	Pitch rate
$\bar{q}$	Dynamic pressure
q_{basis}	NN pitch axis control imput
r	Yaw rate
r_{basis}	NN yaw axis control input

t	Time
u	Pseudo control surface commands
U_{ad}	NN output, augmenting acceleration command
U_{dd}	Research controller PID output
U_{err}	NN adaptation signal
W	NN weights
W_{max}	NN upper weight limit
W_{min}	NN lower weight limit
x	Angular rates
x_{basis}	NN control input
x_{err}	Angular rate error
x_{ref}	Reference angular rate
$\dot{x}$	Angular acceleration
$\dot{x}_c$	Commanded angular acceleration
$\dot{x}_{ref}$	Reference angular acceleration

1. INTRODUCTION

In an effort to improve flight safety and survivability, researchers have been developing new control methods for failure compensation. For example, the NASA Dryden Flight Research Center (DFRC) developed and flight-tested a controller that used propulsion to safely land an aircraft with a disabled primary flight control system (ref. 1). Beyond this example, the search continued for a controller to provide desirable aircraft response over a wide range of unanticipated failures without extensive gain scheduling. To accomplish this, Calise, et al., and Rysdyk, et al. (refs. 2, 3), developed a dynamic inversion controller with direct adaptive neural network (NN) augmentation. This tracking controller adds direct adaptive NNs to a dynamic inversion control law. These NNs are used to generate command augmentation signals to compensate for errors in the estimates from the model inversion because of imperfectly modeled dynamics, as well as dynamics resulting from damage or failure. Simulations of this control method on multiple aircraft (refs. 4, 5) as well as flight tests of the X-36 (Boeing Phantom Works, St. Louis, Missouri) aircraft (ref. 6) show promise for use of this control method to compensate for actuator failures. On the road to developing failure-compensating control methods to improve the safety and survivability of aircraft, NASA created the Intelligent Flight Control System (IFCS) program.

1.1 Project objectives

The objective of the NASA IFCS program is to develop and flight-test control schemes that enhance control during a primary control surface failure. The Gen-2 IFCS flight test project goal is to demonstrate a neural flight control system that can provide adaptive control without the requirement for extensive gain scheduling or explicit parameter identification. The Gen-2 approach requires neither information on the nature or extent of the failure, nor knowledge of the control surface positions in either nominal or off-nominal conditions.

1.2 Adaptive controller design

The Gen-2 approach is based on the augmented model inversion architecture developed by Calise, et al., and Rysdyk, et al. (refs. 2, 3). The general control scheme is based on an adaptive NN controller canceling the errors associated with the dynamic inversion of the model. This control strategy is designed to provide consistent handling qualities without requiring the level of computational and design effort associated with gain-scheduling or classical system identification. The model inversion uses aerodynamic stability and control derivatives determined by previous flight tests with the NF-15B airplane. Desired level-one handling qualities are designated with low-order reference models.

Figure 1 shows the general control architecture. In order to compensate for the angular rate errors (x_{err}), the pseudo control acceleration commands (U_{dd}) are computed by the proportional, integral, and derivative (PID) compensator. Augmenting the baseline controller, pseudo control commands (U_{ad}) are generated by the adaptive NNs.

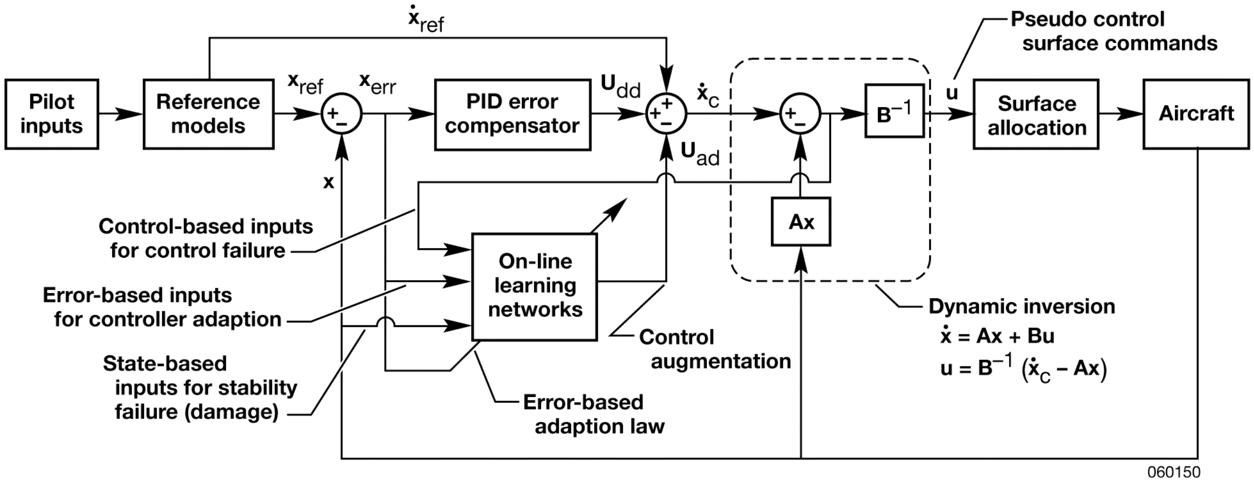

Figure 1. IFCS Gen-2 Control Architecture.

1.2.1 Dynamic inversion

The inputs to dynamic inversion are commanded angular accelerations ($\dot{x}_c$). The control architecture in figure 1 shows a generic dynamic inversion, however, the Gen-2 controller uses a simplified dynamic inversion technique developed by The Boeing Company (ref. 7). The simplified dynamic inversion algorithm is used for pitch and roll axes; however, a classical yaw controller (ref. 8) with lateral acceleration feedback and estimated angular rate of sideslip ($\dot{\beta}$) is substituted for the model reference controller. The three-axis simplified dynamic inversion method with a simulated stabilator lock showed undesirable cross-axis coupling dynamics in the piloted simulation. Although replacing the yaw axis dynamic inversion controller was technically undesirable, because of project schedule pressure, the substitution was made.

1.2.2 Control surface commands

The dynamic inversion algorithm outputs pseudo control surface commands (u). These commands are converted to actual surface commands by a simple allocation. Lateral, longitudinal, and directional commands are sent to the ailerons, differential stabilator, symmetric stabilator, and rudder and differential canard, respectively. This allocation matches that of the conventional controller, as the allocation algorithm was not undertaken as a research area. The symmetric canard is not commanded by the Gen-2 controller; it is scheduled with angle of attack and Mach number, matching the conventional controller.

Damage is simulated by inserting a multiplier in the symmetric canard command loop, independent of the research controller. The canard multiplier effectively changes the apparent aircraft aerodynamics and stability. A failure is simulated by locking a stabilator surface at a trim or off-trim position.

1.2.3 Neural network algorithm

Each axis has a neural network that creates an augmenting angular acceleration command (U_{ad}) for each respective axis. The NNs use proportional and integral rate errors for an adaptation signal (U_{err}) where:

$$U_{err} = \begin{cases} (K_p x_{err} + K_i \int x_{err}) - \varepsilon & \text{when} \quad (K_p x_{err} + K_i \int x_{err}) \geq \varepsilon \\ 0 & \text{when} \quad \left|(K_p x_{err} + K_i \int x_{err})\right| < \varepsilon \\ (K_p x_{err} + K_i \int x_{err}) + \varepsilon & \text{when} \quad (K_p x_{err} + K_i \int x_{err}) \leq \varepsilon \end{cases} \quad (1)$$

K_p and K_i are, respectively, proportional and integral gain vectors for each axis. The adaptation signal gains are not the same as the PID gains in the error compensator, as seen in figure 1. Equation 1 describes how the adaptation signal passes through a dead zone function, which is a nonlinear mapping of near-zero values to zero. Values larger than the tolerance are passed through with a small bias, ε. The dead zone is intended to prevent excessive adaptation when errors are small, which drives the NN weights (W) to a high gain.

The forward NN architecture for the pitch axis is shown in figure 2. The pitch and roll axes have inputs where:

$$x_{basis} = \dot{x}_c - U_{ad} \quad (2)$$

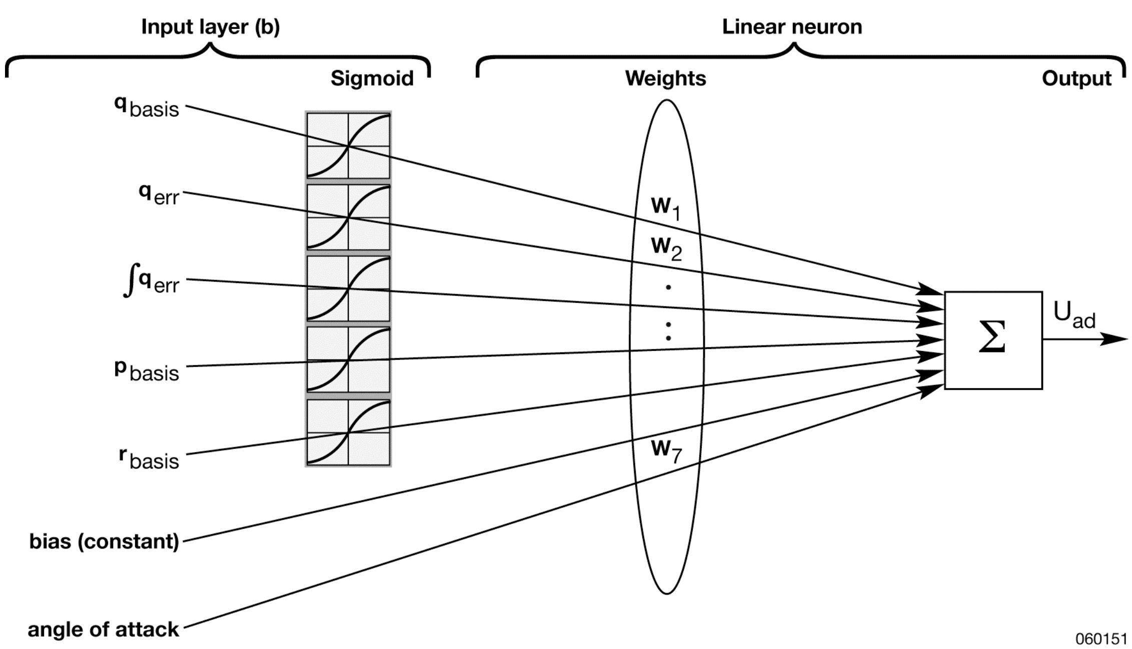

Figure 2. Pitch Neural Network Forward Architecture.

Where the x is p, q, or r (referring to the roll, pitch, and yaw axes, respectively). The cross-axis inputs allow the NN to compensate for dynamic coupling created from a simulated failure. Because of the dynamic inversion redesign (see section 1.2.1), the terms in equation 2 are not used in the yaw axis controller. Therefore, cross-coupling to the yaw axis in the NN has been eliminated by setting r_{basis} to zero.

The NN output is the sum of the product:

$$U_{ad} = W^{\mathrm{T}} b \tag{3}$$

where b is the vector of NN inputs, as seen in figure 2. The output U_{ad} is added to the control command as an angular acceleration command augmentation, as seen in figure 1. The network weights are determined by an adaptation law.

$$\Delta W_i = G_i (L_i \left| U_{err\,i} \right| W_{i_{[k-1]}} + b_i U_{err\,i}) \Delta t \quad , \quad \text{for } i = 1: \text{length}(b) \tag{4}$$

where G and L are user-selected gain vectors, referred to as adaptation gain and learning rate, respectively. Previous frame weights are denoted by $W_{[k-1]}$. Final weights are determined after passing through weight limits specific to each weight.

$$\Delta W_{i_k} = \begin{cases} W_{max_i}, & \text{if } (W_{i_{[k-1]}} - \Delta W_{i_k}) > W_{max_i} \\ W_{min_i}, & \text{if } (W_{i_{[k-1]}} - \Delta W_{i_k}) < W_{min_i} \\ \text{else}, & W_{i_{[k-1]}} - \Delta W_{i_k} \end{cases} \quad , \quad \text{for } i = 1: \text{length}(b) \tag{5}$$

1.3 Aircraft description

As seen in figure 3, the NASA NF-15B airplane is a preproduction F-15B originally built by McDonnell Douglas Aircraft Company, now The Boeing Phantom Works, St. Louis, Missouri, that has been highly modified to support various test programs. The most visible modification is the inclusion of a set of canards near the cockpit. These canards are a set of modified horizontal stabilators from an F-18 (The Boeing Company, Chicago, Illinois) airplane. The propulsion system consists of two Pratt & Whitney (West Palm Beach, Florida) F100-PW-229 engines, each equipped with an axi-symmetric thrust vectoring pitch/yaw balance beam nozzle. Thrust vectoring is not used in the IFCS Gen-2 controller.

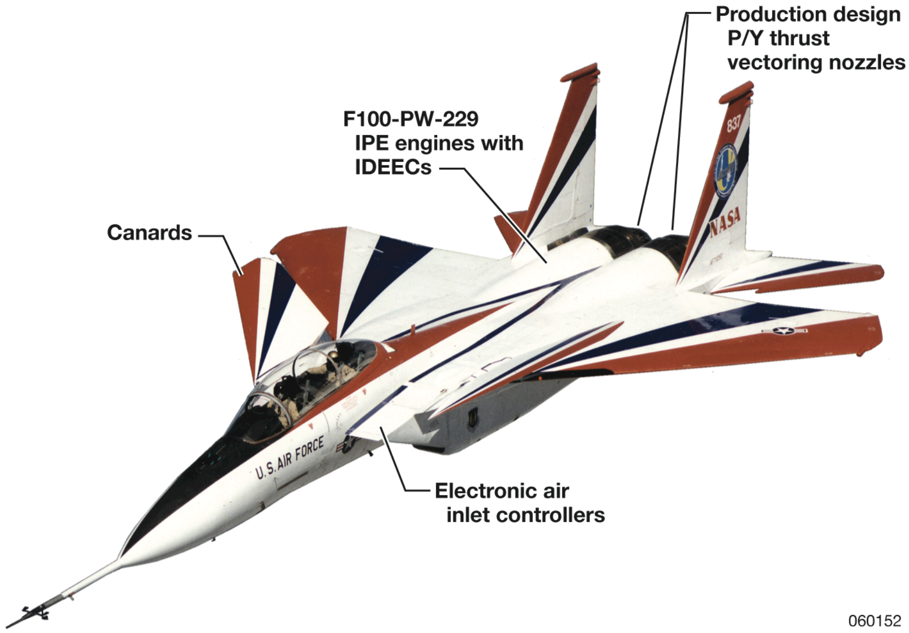

Figure 3. NASA IFCS NF-15B Tail Number 837.

1.3.1 Research computers

The NASA NF-15B is a unique fighter aircraft test bed with legacy research control systems. The legacy system consists of a four-channel flight control computer including four research processors in the Standard Computing Element 3 (SCE-3). The legacy system operates in two modes: conventional and research. The research mode uses commands from the SCE-3, which contains the Gen-2 controller, the simulated failure/damage insertion, the flight envelope monitor, and the NN safety monitor (ref. 9) software. For IFCS, the single-channel Airborne Research Test System (ARTS) II computer replaces a similar research computer. The ARTS II contains the NN algorithm. The SCE-3 communicates to the ARTS II through a 1553 bus.

The flight envelope monitor causes the research mode to transition to conventional mode if any of the monitor parameters exceed their limits. The monitor has an upper and lower limit for the following aircraft state parameters: angle of attack, sideslip angle, pitch angle, bank angle, pitch rate, roll rate, and yaw rate. The monitor has an upper and lower limit for the following flight condition parameters: normal acceleration, lateral acceleration, Mach, dynamic pressure, and altitude. The monitor has an upper and lower limit for the following cockpit condition parameters: pitch stick, roll stick, yaw pedal, and throttle power lever angle. The monitor contains two sets of envelope parameter upper and lower limits. Envelope 1 restricts rates and accelerations for flight-test clearance of less dynamic tests, whereas the parameters of envelope 2 are designed for more dynamic tests.

1.3.2 Pilot-vehicle interface

The control system inherited from previous projects has three pilot-vehicle interfaces (PVI) on the multipurpose display to control research functions. The parameter names are retained, but the parameter functions are modified for IFCS as follows:

- PAL (Pick-A-Limit) selects envelope limits on the SCE-3, envelope 1 or 2;
- DAG (Dial-A-Gain) selects simulated failure/damage on the SCE-3;
- and CAT (Choose-A-Test) selects the flight experiment in the ARTS II, turning the NN algorithm on and off.

With PAL and DAG selections made, the pilot presses the trigger switch to engage the enhanced mode, switching from the conventional controller to the research controller. Next, the CAT selection is made and the nose wheel steering (NWS) button is pressed to latch the CAT value. Subsequent NWS presses will engage research modes dependent on PAL, DAG, and CAT definitions, as seen in figure 4. Anytime the research mode is engaged, a trigger switch press exits research mode, returning to the conventional controller with all test modes (failure or adaptation) disengaged. A 1-second fader between controller commands provides "transient-free" switching.

Test Selected	1st NWS press	2nd NWS press	3rd NWS press	4th NWS press
NN off / failure on	Latch CAT	Failure inserted	Test exited	
NN on / failure off	Latch CAT	NN activated	Test exited	
NN on / failure on	Latch CAT	NN activated	Failure inserted	Test exited

Figure 4. Test Modes by Nose Wheel Steering Button Presses

A paddle switch mounted in front of the stick is provided for emergency exiting of the research mode. The paddle switch reverts the control system to the conventional mode, similar to pressing the trigger switch. However, using the paddle switch sets the master caution and disables the research mode until it is reset by a dedicated switch and button in the cockpit.

Exceeding the envelope limits will automatically disengage the research mode in the same way pressing the paddle switch will. If the envelope limits are exceeded, a failure notice will appear on a multipurpose display.

2. FLIGHT TESTING METHOD

2.1 Structural loads model validation test phase

The Structural Loads Model Validation (SLMV) test phase was added to the IFCS program after determining there was insufficient documentation to support the correctness of the existing structural loads model. Instrumentation was added and ground-calibrated to validate the loads model. The primary objective of the flight test was to obtain enough data to assess the validity of the loads model. Flight conditions were designed to make a grid covering the IFCS envelope. At each flight condition, the following maneuvers were flown: steady-heading sideslips, pitch, roll and yaw doublets, full stick rolls, 4-g windup turns, 4-g loaded rolls and push-over, pull-ups. Once validated, the loads model could be used as a loads preflight prediction tool and a real-time control room monitor for the IFCS Gen-2 flights.

2.1.1 Loads model

The loads model was previously developed by McDonnell Douglas (ref. 10) for the F-15/STOL and maneuvering technology demonstrator legacy program. The development of the loads model had been done using real-time strain measurements from flight. Using aircraft states as inputs, the loads model computes 45 aircraft component loads at 20 load stations (figure 5).

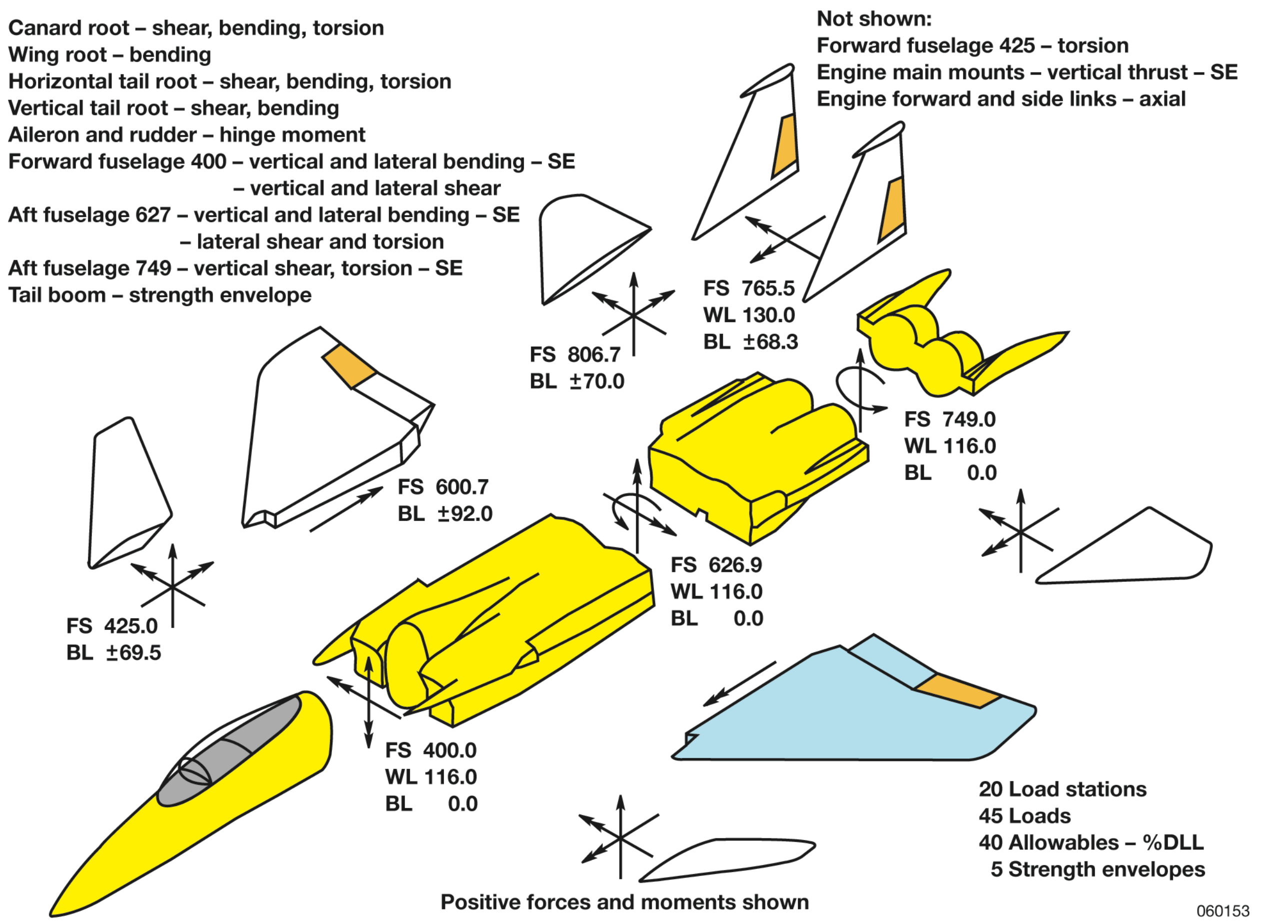

Figure 5. Loads Model Load Stations.

2.1.2 Loads instrumentation added, calibrated, and equations identified

When NASA received the aircraft from McDonnell Douglas, all of the strain gage wiring had been removed. The strain gages still existed in desirable locations and included 63 healthy bridges. These 63 bridges were rewired and an additional 7 bridges were installed on the aircraft for the SLMV test phase.

A full loads calibration was performed in the Flight Loads Laboratory at DFRC. Because of aircraft tie down limitations, the wings were loaded up to 35% design limit load (DLL), the horizontal tails were loaded up to 30% DLL, the vertical tails were loaded up to 22% DLL, and the canards were loaded up to 26% DLL. The strain gage output was assessed for linearity and extrapolated for the higher load levels. The rudders were loaded up to 80% DLL on the aircraft and the aileron actuators were instrumented for hinge moment and loaded to 80% DLL in a load frame machine.

A total of 300 strain gage equations, including primary and backup equations, were identified from the strain gage calibration ground test data. Calibration data showed the left horizontal tail strain gages had very low output and the respective equations had a large root mean square error. Therefore, the left horizontal tail strain gages were not used. A summary of the types of equations that were derived is shown in figure 6.

Surface	Equation Type		
	Bending	Shear	Torque
Left/Right Rudder	X	X	
Left/Right Aileron	X		
Left/Right Wing	X	X	X
Left/Right Canard	X	X	X
Left/Right Vertical Tail	X	X	X
Right Horizontal Tail	X	X	X

Figure 6. Identified Instrumentation Equations.

2.2 Adaptive controller test plan

The NASA NF-15B flight envelope, taken from the Flight Manual Supplement, is shown in figure 7. The IFCS envelope limits altitude and dynamic pressure, not airspeed directly. All test points for Gen-2 are subsonic (at less than Mach 0.95). The Gen-2 controller design did not include supersonic flight conditions to lessen controller design complexity.

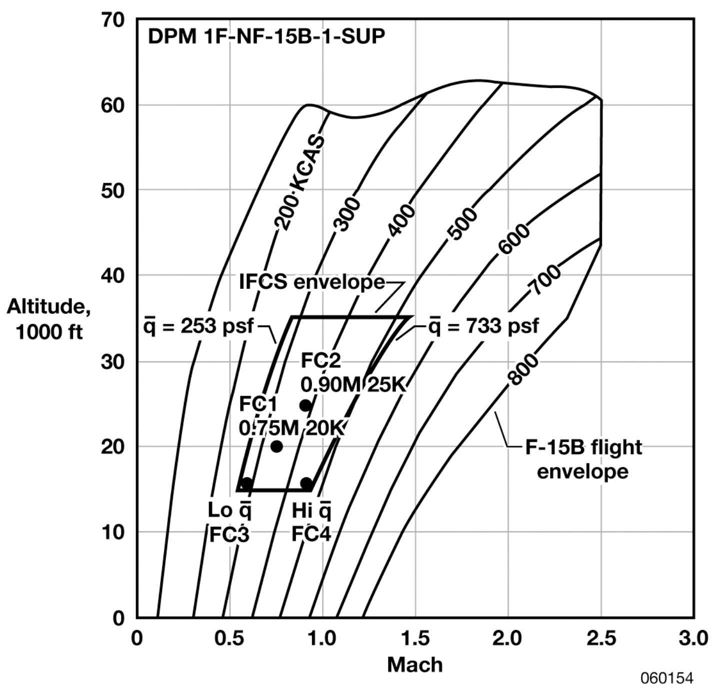

Figure 7. Gen-2 Flight Envelope and Test Conditions.

2.2.1 Envelope clearance approach

A systematic flight test sequence is followed, using a buildup approach, with prior checkout of all test maneuvers in the simulator. Initial flights verify basic functionality of the installed Gen-2 systems. Engage/disengage checks are performed, and the auto-disengage envelope is verified. A standard sequence of maneuver groups are flown, consisting of 1-g clearance maneuvers, followed by a series of basic maneuvering points, and finally a handling qualities research assessment, consisting of 1-g formation flight and 3-g tracking maneuvers.

This sequence is repeated while progressing through the available IFCS configurations: conventional mode, research mode, NN on, simulated failure/damage, and NN on with simulated failure/damage.

In increasing order of severity, the locked stabilator angles from trim are: 0, –2, +2, –4, and +4 degrees. Note that +2 and +4 degree angles are not used in tests due to predictions of aileron saturation during loaded maneuvers. In order of increasing destabilizing effect, the canard gain setting multipliers are: 0.8, 0.6, 0.4, 0.2, 0.1, 0, –0.2, and –0.5. The simulated failures and damage are introduced separately in a buildup sequence. Aircraft response is evaluated using tests of the standard maneuver sequence of 1-g clearance, basic maneuvering, and handling qualities.

Certain maneuvers in this sequence are performed specifically to verify the structural loads model and results developed during the Structural Loads Model Validation phase of the flight program.

2.2.2 Test conditions and maneuver sequence

Four test conditions are indicated within the flight envelope:

- FC1 Mach 0.75 at 20 000 ft altitude
- FC2 Mach 0.90 at 25 000 ft altitude
- FC3 Mach 0.57 at 15 500 ft altitude (near low dynamic pressure limit)
- FC4 Mach 0.92 at 15 500 ft altitude (near high dynamic pressure limit)

The primary flight conditions (FC) during this flight program are FC1 and FC2; FC3 and FC4 are used to clear the research controller at the dynamic pressure limits of the envelope, but not for handling qualities research.

For engagement of a selected test (a PAL/DAG/CAT combination), disciplined clearance procedures using challenge-response commands between the control room staff and the pilot are implemented. The control room staff is required to clearly announce the selections that have been made by the pilot.

The following guidelines are used when developing the test cards to ensure a safe flight test:

- Test cards are verified and initialed by a program engineer (Systems or Flight Controls) to confirm that the test sequences in the test cards are correct.
- Test cards clearly indicate procedures and purpose for each test.
- Test cards are practiced in the simulator prior to flight; this includes identifying the best way to disengage the system.
- The trigger switch is the preferred way to disengage from a test point. The NWS switch is not the preferred way to disengage because this switch has multiple uses and could cause the pilot to confuse the test modes.

The PAL envelope 1 (see section 1.3.1), used first to clear the low dynamic response maneuvers, is followed by envelope 2 to clear higher dynamic response maneuvers. Initial flight tests include checking the mode logic and insipient dynamics when engaging or disengaging, both initiated by the pilot and initiated automatically (for example, when the envelope is exceeded). The maneuver descriptions include:

- **Loads signature maneuver**

  Mission rule number 25 states, "All Gen-2 maneuvers will be flown with and without surface failures prior to turning on adaptation to assess the validity of the loads model. A loads signature maneuver will be flown prior to IFCS." This mission rule required postflight processing of the loads data, comparing the loads model to the instrumented loads. In each flight, prior to Gen-2 test points, a loads signature maneuver was flown to assess the health of the instrumented loads as well as the health of the real-time control room loads model. The loads signature maneuver included flying pitch, roll and yaw doublets, left and right full-stick rolls, and left and right 3-g windup turns (WUT). It was flown at 20 000 ft and Mach 0.75 (at FC1). If the loads model or the instrumented loads were not working properly, the issue was addressed and the decision was made to either continue with the Gen-2 test points or return to base and troubleshoot the problem on the ground.

- **1-g clearance**

  The 1-g clearance test block consists of standard maneuvers designed to give the pilots and engineers a qualitative feel for aircraft performance at a specific test condition. These maneuvers are accomplished prior to more aggressive maneuvers in order to judge aircraft response and dynamics. The 1-g clearance maneuvers do not have tolerances associated with them.

  Pitch, roll, and yaw stick and pedal raps are performed from a trimmed, 1-g flight condition. The success criterion is pilot and engineer assessment of acceptable aircraft response and dynamics, particularly aeroservoelastic excitation. Pitch, roll, and yaw doublets are performed from a trimmed 1-g flight condition. Bank-to-bank rolls and pitch attitude captures are performed separately per the pilot's satisfaction up to 60 degrees bank angle and 30 degrees pitch angle.

- **Basic maneuvering**

  The basic maneuvering test block consists of higher dynamic response maneuvers. These maneuvers include 360-degree rolls performed with a half or full stick input (depending on predicted structural loads), steady heading sideslips, and slow onset WUT to 3-g. This test block complements the 1-g clearance test block in clearing a specific part of the envelope for research maneuvers. The criterion for success is pilot and engineer assessment of acceptable aircraft response.

- **Handling qualities research maneuvers**

  The 1-g formation flight and 3-g tracking evaluations involve the test aircraft using the chase aircraft as an air-to-air reference during pilot assessment of handling characteristics during handling qualities tasks. Figures 8 and 9 show the qualitative checklists for the 1-g formation flight and 3-g tracking tasks, respectively. The pilot performs the task according to the "desired" and "adequate" criteria. Immediately after the task is completed, the pilot completes the "pilot comments" section, giving his assessment for each item, concluding with Cooper-Harper ratings for gross acquisition and fine tracking, a Pilot-Induced Oscillation (PIO) rating, and an overall confidence rating of his assessment.

IFPC MODE SW – ENHAN

TRIGGER ON (ENHAN)

FORMATION FLIGHT
DESIRED: WITHIN FWD CANOPY RING AND EJECTION SEAT 75%
ADEQUATE: WITHIN 1 CANOPY DIM UP OR DOWN 100%
PILOT COMMENTS:
CONTROL:
INITIAL RESPONSE
UNDESIRABLE MOTIONS
PREDICTABILITY
DIFF W/GROSS ACQUISITION
AGGRESSIVENESS EFFECTS H/Q
COMPENSATION TECHNIQUES
PERFORMANCE
ADEQUACY OF PERFORMANCE
COUPLING OF AXES
SENSITIVITY
FEEL SYSTEM:
FORCES
CONTROL MOTION
HARMONY
NONLINEARITY
FRICTION AND BREAKOUT

TRIGGER OFF (CONV)

IFPC MODE SW – CONV

GROSS ACQ HQR_____ FINE TRACKING HQR_____
PIO RATING ______ CONFIDENCE RATING _______
060155

Figure 8. 1-g Formation Flight Handling Qualities Assessment.

IFPC MODE SW – ENHAN

TRIGGER ON (ENHAN)

LONGITUDINAL TRACKING – 55MIL RET
1000 – 1500 FT IN TRAIL
TARGET: 3 – G
ACQ DESIRED: +/– 25 MILS & 1 O/S
ACQ ADEQUATE: +/– 50 MILS & 2 O/S
FINE DESIRED: +/– 5 MILS 75%
FINE ADEQUATE: +/– 10 MILS 100%
PILOT COMMENTS:
CONTROL:
INITIAL RESPONSE
UNDESIRABLE MOTIONS
PREDICTABILITY
DIFF W/GROSS ACQUISITION
AGGRESSIVENESS EFFECTS H/Q
COMPENSATION TECHNIQUES
PERFORMANCE
ADEQUACY OF PERFORMANCE
COUPLING OF AXES
SENSITIVITY
FEEL SYSTEM:
FORCES
CONTROL MOTION
HARMONY
NONLINEARITY
FRICTION AND BREAKOUT

TRIGGER OFF (CONV)

IFPC MODE SW – CONV

GROSS ACQ HQR_____ FINE TRACKING HQR_____
PIO RATING ______ CONFIDENCE RATING _______
060156

Figure 9. 3-g Tracking Task Handling Qualities Assessment.

2.3 Piloted nonlinear simulation for risk reduction

The closed-loop simulation testing is done at the DFRC six-degree-of-freedom, flight-validated, nonlinear simulator (ref. 8). Fixed-base real-time piloted flight and batch operation modes are available and are both used for validation and verification of the research systems. Locked actuator failures are modeled by overriding controller commands on any single control surface.

By mission rule, pilots are required to simulate every test card prior to flight test. Mission rule number 22 for the IFCS project states, "All research maneuvers will be flown in the simulator prior to flight. Maneuvers with unacceptable handling qualities or transient characteristics will NOT be flown." Generally, the day prior to the scheduled flight test, the mission pilot would fly in simulation to familiarize himself with the maneuvers and predicted dynamics, especially with respect to failure or damage insertion and trigger disengagement of the research controller during maneuvering. This process adds efficiency and safety for the flight test. Flight test planners are able to assess and modify how the pilot executes the test. Also, this predictive data runs the structural loads model to ensure loads are within limits.

Mission rule number 23 for the IFCS project states, "The maximum loads seen during simulation will be briefed before each flight." After the simulation was complete, a summary of the maximum loads for each flight card were compiled and presented at the crew briefing before each flight. In some cases, when the flight included test cards previously flown, actual flight data, including instrumented loads, was presented at the crew briefing.

2.4 Control room monitoring

Monitoring flight data in the control room is done primarily to ensure the safety of flight. With this in mind, a series of mission rules were established to ensure a safe flight.

2.4.1 Structural loads

Mission rule number 26 states, “In the event that 100% DLL is exceeded, the pilot will select conventional mode and a ‘Return to Base’ will be initiated immediately.” If a load exceeds 100% DLL based on either the loads model or the instrumented load, the aircraft is to land and an inspection of the overloaded location is to be conducted.

Flight safety was facilitated by monitoring loads in real time on a series of displays in the control room. In addition to monitoring instrumented loads, engineers incorporated the loads model into the control room displays using the real-time aircraft parameters for inputs to the model. The displays included two displays to check the health of the strain gages on the ground prior to flight. The strain gage zeros display shows the output of all strain gages. If the output is within a ±1% of full-scale range for each individual strain gage, it is said to be healthy. If the output is outside of this range, the value turns red. The strain gage resistance calibration display looks the same as the zeros display and will also alert the control room if the output is outside ±1% of the full-scale range of the resistance calibration value for each individual strain gage by turning the value red.

During flight, a series of four displays are monitored. Two of these displays include bar charts that show the absolute magnitude of each load from both the loads model and the instrumented load; figure 10 shows the loads model bar chart. Warning colors are assigned to increasing DLL values to draw the attention of the engineer. In the event of an overload, the engineer is able to make a direct abort call to the pilot. The pilot would return the aircraft to level 1-g flight and select conventional mode. The final two displays monitored during flight are time histories of the same data included in the bar chart displays. The time history displays allow the engineer to monitor trends and also scroll back through the history to review maneuver loads.

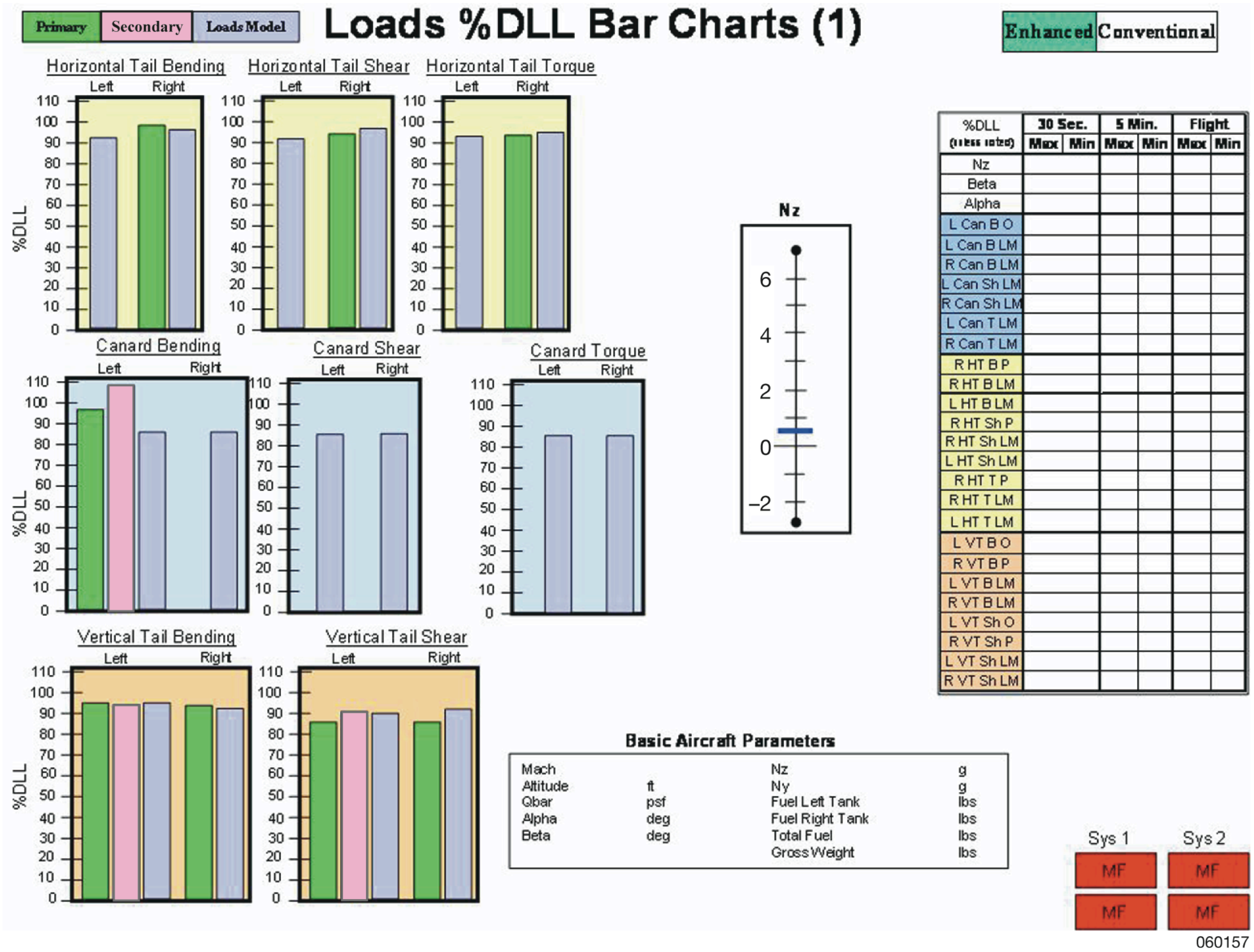

Figure 10. Loads Model Bar Chart Display.

2.4.2 Flight controls and dynamics

Control room monitoring for flight controls and dynamics is done in two categories: test mode change transients, and neural network learning. With the many test modes (i.e. research, conventional, simulated failure/damage, and adaptation), there exist many possible false predictions from simulation of the aircraft dynamics. Control room staff monitor the transient-free requirement of $\pm 2g$ longitudinal and $\pm 0.5g$ directional accelerations during engagement and disengagement of the research controller. The prediction of longitudinal acceleration from simulation data after insertion of failure/damage information is printed on the test cards for quick comparison during flight. When the canard multiplier and stabilator locks are introduced and after trimmed flight is recovered, trim states (such as angle of attack and sideslip angle) and surface positions are compared to a reference table derived from simulation. During loaded rolls with a simulated failure, control surface allocation can move the ailerons to their maximum deflection. Therefore, attention is given to aileron position during maneuvers with simulated failures and an “abort test” call would be made in the event of saturation.

Control room monitoring of NN behavior has two objectives: maintaining flight safety by disallowing unstable learning, and allowing adaptation to occur to collect the desired research. Flight safety largely depends on the automatic mode disengagements and the pilot’s ability to disengage the test according to his comfort with controller behavior.

Tolerances for acceptable NN learning are difficult to define, and therefore were dependent on engineer assessment of the real-time NN command augmentation and weights relative to pilot inputs and qualitatively compared to simulation predictions. A notebook of simulation recordings of these parameters is available for reference in the control room for each test mode. Engineers use these predictions to estimate which weights will be the most active and achieve the largest magnitude for a specific test, such as which weights are predicted to reach a limit. Large changes in oscillatory weights or weights that change sign are known from observation in simulation to be unsatisfactory NN behaviors and therefore would prompt engineers to call for test abort. The reasons for calling a test abort are summarized in mission rule number 21 that states, “The neural network parameters will be monitored in the control room for consistency with simulation predictions. If poor trending is observed, ‘ABORT, ABORT, ABORT’ shall be called.”

Figure 11 shows the control room display NN tab, which contains strip charts for pilot inputs, NN augmentation command, research controller PID command, and normalized NN weights. Below the strip charts are digital readouts of the NN weights and “StopLearn” flags for each axis.

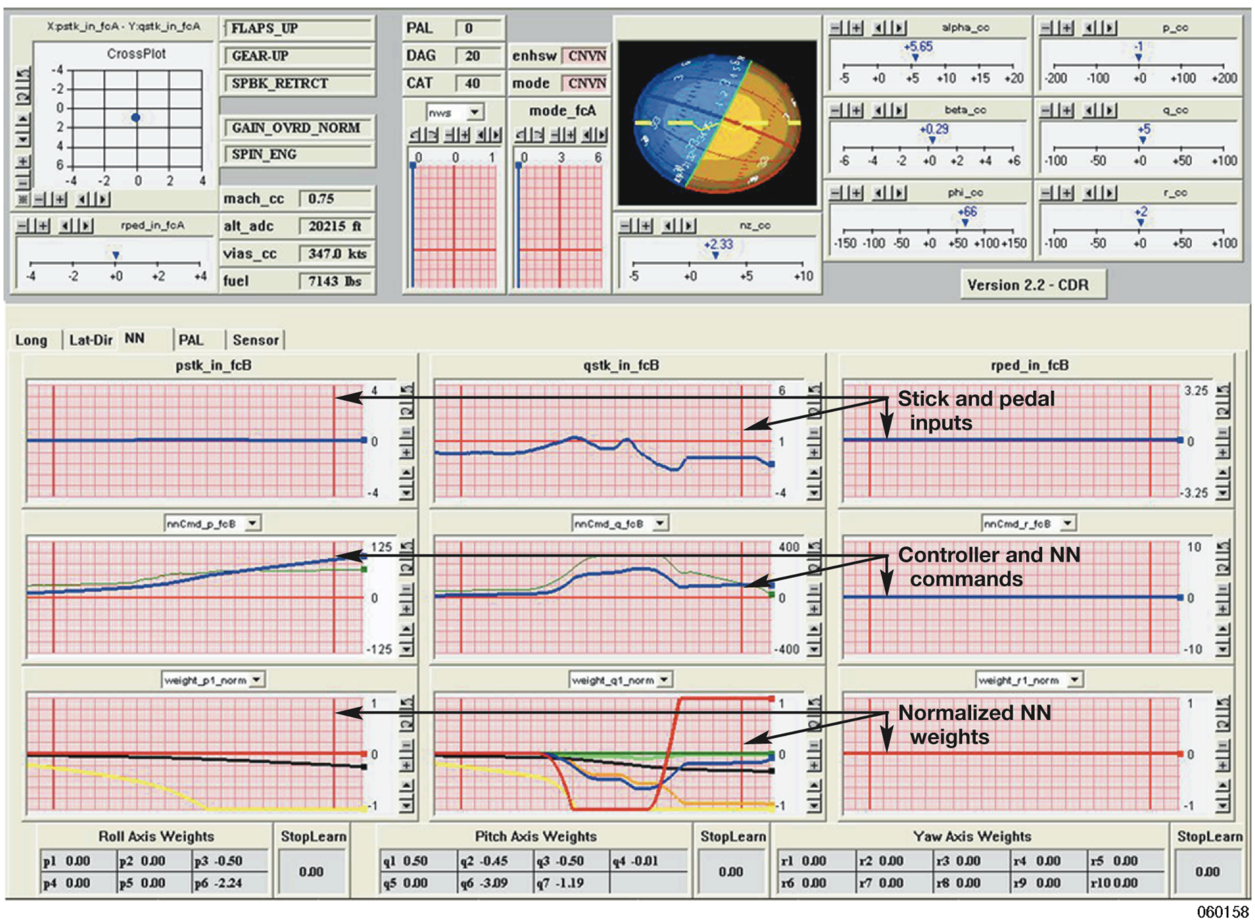

Figure 11. Flight Controls and Dynamics Control Room Display for NN Monitoring.

3. RESULTS

3.1 Structural loads model validation flight test results

A total of six flights were dedicated to loads model validation. Fifteen subsonic flight conditions were flown. The loads model output was monitored and compared to instrumentation in real time in the control room. To validate the model, each loads model output was compared to instrumented loads, examining how well the trends were matching, and quantifying the loads model offset from instrumented load. A comparison of loads model output to instrumented load was made on the canards, wings, ailerons, rudders, vertical tails, and horizontal tails.

Comparing flight data showed that the largest difference was a 30% DLL. This large discrepancy was attributed to the aileron hinge moment, with the model underpredicting the instrument output. The trends for the aileron comparison, however, matched well.

Comparing the loads model output to the instrumentation output showed that the rudder comparison was not a direct comparison. The loads model computed hinge moment while the instrumentation measured bending. The rudder, therefore, was not validated, but was considered to be a less critical load for the IFCS program, since the rudder loads were predicted by the loads model to be less than 50% DLL for all flight maneuvers.

For validation of the right horizontal tail, the bending and shear comparisons matched well to instrumented loads, although the torsion comparison did not match well. The right horizontal tail torsion instrumentation showed low load during flight and therefore was determined to be a less critical load for the IFCS program.

The shear and torque on the left canard, and shear, bending, and torque on the right canard did not give good matches. Revisiting the strain gage calibration, it was found that some strain gages used in the loads equations had large nonlinearities. The left canard shear and torque instrumentation and all right canard instrumentation was determined inoperative and was not used in the validation. The left canard bending comparison showed a good match and provided confidence that the loads model predictions were correct and should be used when predicting Gen-2 flight test loads.

Finishing the comparisons, it was determined that the vertical tail loads model output overpredicts at higher loads and that the wing bending comparison matched well.

With the knowledge gained from the SLMV flight test, it was concluded that the loads model was validated and acceptable for future flight test. A limit was set that the IFCS program would not fly any maneuvers that would exceed 70% DLL based on preflight simulation loads model output. This 70% DLL limit for the model output covered the worst-case aileron hinge moment under-prediction, thus predicting 100% DLL from instrumentation would not be exceeded during flight. With this validation data, the loads model was then used as a loads preflight prediction tool and a real-time control room display for the IFCS Gen-2 flights.

3.2 Gen-2 test execution

Eighteen Gen-2 flights were conducted over approximately 4 months. The buildup envelope clearance was successfully executed. Initial flights verified basic Gen-2 system functionality. Performing stick raps around the envelope cleared the Gen-2 controller with respect to aeroservoelastic concerns in two flights: the second flight and the sixth flight (finishing the high dynamic pressure points). To partially verify the PAL logic, the second flight included testing the automatic disengagement of the research controller resulting from exceeding the PAL envelope limits for low altitude and low dynamic pressure. Disengagements of the research controller occurred with insignificant dynamic transients. On the third flight, NN software was successfully engaged for the first time, with very small contributions from adaptation as predicted in a no-failure configuration.

Engagement and manual disengagement of the research controller proved transient-free as designed. Transient-free controller switching was demonstrated for all failures and during all maneuvers. Pilots gained confidence in the transient-free switching to the point of commenting that continuing to check disengagements was not necessary.

Clearance of canard multipliers from +0.8 to +0.2 was completed in the third and fourth flights, allowing the first handling qualities research with simulated damage to commence on the fifth flight. Both pilots rated the failure handling qualities as better with the adaptation on than off, demonstrating in flight test that the adaptive controller could improve handling qualities, thus meeting a project milestone.

Clearance continued for canard multipliers from +0.1 to –0.5 with subsequent handling qualities evaluations with the –0.5 canard multiplier. The larger simulated damage was not as effective in degrading aerodynamic stability as desired; the simulator had over-predicted the effect of the canard multiplier. Therefore, the largest canard multiplier did not lower the handling qualities ratings to level 3, but only level 2.

The simulated stabilator-locked failure clearance was then conducted, followed by handling qualities research for 0, –2, and –4 degrees from trim cases.

3.2.1 Adherence to the test plan

Envelope clearance for FC1 was executed successfully with some modification. The 3-g WUT maneuver was designed to clear the aircraft response for the 3-g handling qualities testing. On the fourth flight, a handling qualities 3-g tracking maneuver was executed in conventional mode. Jet wash was encountered, causing a peak of 4.6g. This event and pilots' comments of needing more maneuver freedom with respect to the tracking task caused the project team to change the basic maneuvering clearance card to replace the 3-g WUT with a 4-g WUT.

With the experience at FC1, the FC2 buildup was shortened for the canard multiplier. Flight condition 2 canard multiplier buildup was modified to clear only 0.2, 0, –0.2, and –0.5 multipliers. This buildup was determined safe after analyzing the FC1 data, which showed a destabilizing effect of the canard multipliers that was less than predicted. This approach provided direct comparison of FC2 to FC1 handling qualities ratings for 0.2 and –0.5 multipliers.

Clearance at FC2 with NNs off was accomplished on the sixteenth and seventeenth flights, followed by handling qualities ratings on the eighteenth and last flight. Clearance of NNs on at FC2 is tabled until an approach to structural load limits is modified to ensure that load predictions fall within limits. This requires raising the acceptable load limit for loads where the current 70% DLL limit is overly conservative. Tabling FC2 with NN on for further analysis of loads limits was planned prior to starting this phase of flights.

3.2.2 Aileron saturation

During the eighth flight on a disengage test card, the 3-g loaded reversal maneuver was executed. The trigger switch disengaged at wings level flight with the research controller in the NN on position and a 0-degree stabilator failure. With slightly more than half stick input on the reversal (2.3 out of 4 inches), the aileron saturated at slightly less than 20 degrees for about 1 second before the trigger was pressed. Aileron saturation did not occur in the piloted simulation because only the left reversal direction was simulated, not the right, which was the worst case. The transient-free switching was flawless, however, several procedures were changed as a result of this incident.

The loaded reversal maneuver was part of testing transients resulting from disengagement. A loaded reversal in research mode was not included in the list of maneuver clearance tests that are executed before disengage transient tests. To remedy the clearance procedure, 3-g loaded reversal maneuvers were added to the basic maneuvering test card to clear the maneuver before clearing the disengage transient test.

Because of the asymmetry associated with the stabilator failure, all turn maneuvers with a stabilator failure are flown in both directions. Mission rule number 22 was violated since this exact turning maneuver was not executed in the piloted simulation before flight test. This mission rule was emphasized to the engineers and pilots involved and warning indicator in the simulation was added to alert the engineers and pilots if surfaces approach saturation.

3.2.3 Pilot-vehicle interface (PVI) confusion

Having inherited the research systems from previous projects (see section 1.3.2), the IFCS team acknowledged the difficulties in using the defined PVI. The project decided, however, that the PVI had acceptable flexibility to meet the IFCS requirements and a PVI redesign was out of the project scope.

During one flight, after completing the standard maneuvers, the test card instructs the pilot to “trigger off” to disengage the research mode, which, on this card, included the NN and failure. Instead of pressing the trigger switch, the pilot mistakenly and unaware of his actions, used the NWS button, disengaging the NN and failure, but remaining in the research mode. The control room staff failed to notice the indication on their control room displays. Moving on to the next test card, the pilot was instructed to “trigger on”. The pilot depressed the trigger and noticed he was now in conventional mode. Knowing he was supposed to be engaging the research mode, he thought he had mistakenly pressed the trigger switch twice; hence he depressed the trigger again, now engaging the research mode. Control room staff noticed the multiple trigger switch depressions along with comments about mode switching from the pilot and control room staff then paused, looked back at the data, and determined the actual events. After clarifying between the pilot and control room what had occurred, testing continued. The confusing PVI design was known prior to this event, however, control room staff failing to catch the mistake immediately led to further confusion, compromising situational awareness for the pilot and control room staff. No maneuvering was conducted during the event and all actions were clarified within a minute after the testing continued.

3.3 Predictions versus results

3.3.1 Failure/damage simulation

Simulated failure/damage did not have as adverse an affect on handling qualities as expected. Canard multipliers did not destabilize the airplane as simulation predicted. The largest damage simulation of a -0.5 canard multiplier in flight test equated approximately to the simulator prediction for a 0.1 canard multiplier. Handling qualities ratings were expected to reach level 3 of the Cooper-Harper rating scale, but pilots’ worst ratings were level 2 for the canard multiplier damage simulation. Aerodynamic modifications to the simulator were undertaken after this flight phase to improve predictions. Software modification to include larger multipliers for the canard was undertaken after this flight phase as well.

Stabilator lock simulated failures were rated at level 1 or 2 Cooper-Harper. Pilot-induced oscillation ratings ranged from 2 to 4 and were often the more noticeable objection. The better-than-expected handling qualities for these failures is conjectured to result from pilot adaptation to the cross-axis coupling dynamics, as the pilots naturally changed their stick inputs based on the aircraft dynamics. Future work includes modification to the handling qualities tasks to make the task more demanding and compromise the pilots' own adaptation to the failure.

3.3.2 Neural network adaptation

As expected, NN adaptation followed simulator-predicted trends but not exact values. Neural network weights in simulation are different from those in flight because small differences between simulation models and flight dynamics have significant effects on adaptation. In this aspect, the NN adaptation is similar to an integrator, where small differences can add up to large differences.

With respect to improving handling qualities, the adaptation had mixed results. Generally, the error reduction provided by the NN resulted in:

- improved gross acquisition ratings
- more PIO tendencies that adversely affected fine tracking ratings

The adaptation effect on cross-axis coupling dynamics tended to improve longitudinal dynamics and worsen lateral dynamics. A study of piloting technique and the resultant NN adaptation was undertaken after this flight phase. Despite mixed results, the flight test demonstrated that adaptation provided some improved dynamics that had trending similar to simulation predictions. Equally important, flight test uncovered unknown deficiencies in the NN design. Future work includes addressing the inability to demonstrate these deficiencies with the current simulation testing and modifying the NN algorithm to address the deficiencies.

During the aileron saturation occurrence (see section 3.2.2), the neural networks adapted very quickly to accomplish an unachievable roll rate. This was a known deficiency in the NNs and therefore protection was included in the NNs to stop learning when a surface saturates. However, the stop learning logic used a value of 20 degrees for the aileron position limit and the value passed to the stop learning logic was only maximum 19.8 degrees. The stop learning was not engaged as intended for surface saturation. A change to the limit is planned for a future software release. Also, the NN adaptation during this maneuver was considered poor by control room staff, and a test abort call would have been made if the pilot had not already disengaged the test.

3.3.3 Loads model and instrumented loads

Postflight data are used to continue validation of the loads model with the Gen-2 controller and simulated failure/damage. The loads model output from flight is compared to both the simulated loads model output and the instrumented loads output. From this three-way comparison, bias can be added to the simulation loads model to better predict in-flight loads.

Flight data trends show that the real-time loads model produces 15% DLL larger canard loads, 10% DLL larger wing and horizontal tail loads, and 25% DLL larger aileron loads than in the simulation. Instrumented loads confirm the in-flight loads model data. The maximum 70% DLL requirement for simulation prediction gave sufficient margin to ensure that 100% DLL was not exceeded during flight.

After analyzing all of the input parameters that contribute to the loads model for both simulation and in real time, it was determined that the simulation was predicting a smaller angle of attack than what actually occurs in flight. This difference in angle of attack produces smaller loads in the simulation loads model than in the real-time loads model.

4. CONCLUSIONS

The method for flight-testing the Intelligent Flight Control System Gen-2 project on the NASA NF-15B airplane proved successful. The project objectives were mostly completed. A small design compromise was made with respect to testing a dynamic inversion controller, yet, the focus on demonstrating the improvements from the direct adaptive neural network in the presence of simulated failure/damage was accomplished.

Structural loading was addressed with the precluding loads calibration ground testing and dedicated flight testing phase. The flight data gathered validated the loads model, which was used for Gen-2 flight test planning.

Flight-testing continued with the Gen-2 controller, using test maneuvers in a sequenced approach for clearance of the new controller with respect to dynamic response, simulated failure/damage, and adaptation on and off. This buildup approach was slightly modified because of flight results, but generally proved to be appropriately cautious for the clearance of all test modes. Control room monitoring of loads sensors, flight dynamics, and controller adaptation followed by postflight data comparison to simulation ensured a safe methodology of buildup testing.

A handling qualities evaluation was conducted on the capability of the Gen-2 controller to restore aircraft response in the presence of a simulated failure/damage. Results from this evaluation were mixed, giving reason for future work on handling qualities task definition, neural network design, and simulation improvements.

This phase of flight-testing the IFCS Gen-2 system was completed without major incident, successfully uncovering strengths and weaknesses of the Gen-2 control approach in flight.

5. LESSONS LEARNED

5.1 Flight planning

The many failure/damage, adaptation on/off, and research/conventional mode combinations possible along with the clearance and handling qualities flight test maneuvers created a large test set. Rigorous attention to details of the buildup approach, including data analysis, successfully provided flight test safety. The flight planning remained flexible, allowing small modifications to the plan from experience and data gained. This was possible with the team focused on the flight safety approach, not only on specific tests.

Simulation predicted worse dynamics than were encountered in flight. Therefore, the buildup approach for simulated damage at FC1 was overly conservative and hence modified for FC2. Even with the many failure/damage test capabilities, the testing would have been more useful if 1) the canard multipliers covered a larger range, beyond what the simulator predicted as safe, or 2) the software for the canard multipliers was quickly modifiable (for example, in less than 1 week). The capability to flight test the failure/damage before the Gen-2 controller experiment to quantify aerodynamic effects would have been useful for designing the test and for better simulator prediction.

5.2 Parameter verification and validation

The loads model requires a total of 38 input parameters. It was determined from flight test data that some of the input parameters chosen, such as angle of attack, angle of sideslip, and axial accelerations were not corrected to take into account the location of the sensor. This introduced some slight offsets in the output loads at some load stations. Some corrected parameters were swapped for the real-time model, while others were corrected post flight. For parameters that were corrected post flight, it was determined that the effect of using the raw sensor output was small and the corrected parameter was not easily available. The lesson learned is to double-check the source and location of the sensors that are used as inputs to a flight safety tool. Incorrect input parameters gave erroneous load output that raised unwarranted flags during flight test.

5.3 Control room monitoring

Real-time monitoring in the control room is an essential part of maintaining flight safety. A backup engineer was tasked to monitor loads and was temporarily confused as to which displays are critical to monitor. As a corrective action, the structures lead engineer will write a control room procedure for the structures discipline that outlines the responsibilities of the engineer monitoring the flight, specifically which displays need to be monitored on the ground and during flight. The document will also include the objectives of loads monitoring for the particular phase of flights as well as actions that will be taken if limits are exceeded during flight.

The PVI was known to have a deficiency as described in section 2.2.2, "The NWS switch is not the preferred way to disengage because this switch has multiple uses and could cause the pilot to confuse the test modes." Control room displays did not place emphasis on drawing attention to the use of the NWS for disengaging the research mode, however. Hence, there was an occurrence that didn't directly jeopardize flight safety, but lowered situational awareness of the pilot and control room as described in section 3.2. This known concern should have been better addressed through control room displays that directly alert the team of a NWS switch disengagement.

6. ACKNOWLEDGEMENTS

The IFCS team consists of the NASA Dryden Flight Research Center, the NASA Ames Research Center, The Boeing Company Phantom Works in St. Louis, MO, The Institute for Software Research in Fairmont, WV, and West Virginia University in Morgantown, WV. Thanks to the many colleagues whose work is herein described.

7. REFERENCES

1. Burken J., et al., *Flight Test of a Propulsion Based Emergency Control System on the MD-11 Airplane with Emphasis on the Lateral Axis*, NASA/TM-4746, July 1996.

2. Calise A.J., Lee S., Sharma M., "Direct Adaptive Reconfigurable Control of a Tailless Fighter Aircraft," AIAA Paper 98-4108, *AIAA Guidance, Navigation, and Control Conference and Exhibit,* Boston, Massachusetts, August 14–17, 1998.

3. Rysdyk R.T., Calise A. J., "Fault Tolerant Flight Control via Adaptive Neural Network Augmentation," AIAA Paper 98-4483, Boston, Massachusetts, August 1998.

4. Kaneshige J., Bull J., Totah J.J., "Generic Neural Flight Control and Autopilot System," AIAA Paper 2000-4281, *AIAA Guidance, Navigation, and Control Conference*, Denver, Colorado, August 14–17, 2000.

5. Kaneshige J., Gundy-Burlet K., "Integrated Neural Flight and Propulsion Control System," AIAA Paper 2001-4386, August 2001.

6. Brinker J., Wise K., "Flight Testing of a Reconfigurable Flight Control Law on the X-36 Tailless Fighter Aircraft," AIAA Paper 2000-3941, *AIAA Guidance, Navigation, and Control Conference*, Denver, Colorado, August 14–17, 2000.

7. Buckley, James, *Versatile Flight Control System Functional Description Active Application*, McDonnell Douglas Corporation, 1995.

8. Burken, John J., Peggy Williams-Hayes, John T. Kaneshige, Susan J. Stachowiak, *Reconfigurable Control with Neural Network Augmentation for a Modified F-15 Aircraft*, section "Classical Yaw Axis Controller," NASA/TM-2006-213678, April 2006.

9. Perhinschi, Mario G., Marcello R. Napolitano, Giampiero Campa, Heather E. Burke, Richard R. Larson, John Burken, and Mario L. Fravolini, "Design and Testing of a Safety Monitor Scheme on the NASA Gen 2 IFCS F-15 Flight Simulator," AIAA Paper 2004-6284, *AIAA 1st Intelligent Systems Technical Conference*, Chicago, Illinois, September 20–22, 2004.

10. McDonnell Douglas Aerospace, *ACTIVE Loads Prediction Program (ACTIVE_FLY) Users Manual*, Revision E, June 9, 1998.

11. *Flying Qualities of Piloted Vehicles*, MIL-STD-1797, March 31, 1987.

12. Norlin, Ken, *Flight Simulation Software at NASA Dryden Flight Research Center*, NASA/TM-104315, October 1995.

8. AUTHORS' BIOGRAPHY

Mark Buschbacher graduated in 1997 from the University of Michigan in Ann Arbor with a B.S.E. degree in Aerospace Engineering. Before finishing his undergraduate, he started his aerospace career as a co-operative student at NASA Dryden Flight Research Center. Upon undergraduate completion, he spent 1½ years as a Delta II rocket scientist for The Boeing Company in Huntington Beach, CA. Upon returning to NASA Dryden in 1999, Mark worked on several projects as an aerospace engineer in the Flight Controls and Dynamics branch. Taking a sabbatical from Dryden, Mark graduated in 2004 from the University of California, Irvine with a M.S. in Mechanical and Aerospace Engineering. After returning, Mark continued to work on the IFCS Gen-2 project as controller designer and analyzer, flight test planner and data analyzer, and flight controls group leader. A capstone of approximately 4 years of work, the IFCS Gen-2 is the first of hopefully many projects for him to flight test.

Heather Maliska graduated in 1999 from the University of Wisconsin-Madison with a B.S. degree in Mechanical Engineering. In 1998 she was a participant of the NASA Academy at NASA Dryden Flight Research Center. Upon undergraduate completion, she returned to NASA Dryden in the Aerostructures Branch. Heather has worked in the Aerostructural Loads group for 7 years and has focused her efforts on ground loads calibration testing and flight testing. In addition to working on the IFCS project, Heather has also worked on the Aerostructures Test Wing, and the X-38, and Active Aeroelastic Wing projects.